Applied Catalysis B: Environmental 185 (2016) 233–241

Contents lists available at ScienceDirect

Applied Catalysis B: Environmental

journal homepage: www.elsevier.com/locate/apcatb

Hydrogen generation via catalytic partial dehydrogenation of gasoline and diesel fuels

Elia Gianotti, Mélanie Taillades-Jacquin*, Álvaro Reyes-Carmona, Gilles Taillades, Jacques Rozière, Deborah J. Jones

Institut Charles Gerhardt UMR 5253, Agrégats, Interfaces et Matériaux pour l'Energie, Université de Montpellier, Place Eugène Bataillon, 34095 Montpellier Cedex 5, France

ARTICLE INFO

Article history:
Received 23 July 2015
Received in revised form 1 December 2015
Accepted 10 December 2015
Available online 12 December 2015

Keywords:
Hydrogen production
Catalytic partial dehydrogenation
Gasoline
Diesel

ABSTRACT

Partial dehydrogenation (PDh) of fuels is a novel method to generate high purity hydrogen on-board, in order to directly feed a fuel-cell based power unit. In this work, the PDh of diesel and gasoline has been studied in order to investigate the possibility of applying such a system to vehicles. The studies have been performed with a Pt–Sn/γ-Al_2O_3 catalyst using a series of diesel and gasoline surrogates. The reactivity of the fuels has been studied, identifying different reaction mechanisms, in relation to the chemical composition and the process conditions. The PDh of a gasoline surrogate provides an average hydrogen production of 1800 NL h^{-1} $kg_{cat}{}^{-1}$ with a purity of over 99% vol. and an extrapolated catalyst lifetime of over 300 h. With diesel, PDh gave an average hydrogen production of 3500 NL h^{-1} $kg_{cat}{}^{-1}$, a purity of over 99% vol. and a lifetime of only 29 h. These preliminary results open up interesting perspectives for future applications of the partial dehydrogenation technology to feed on-board fuel-cells.

1. Introduction

The control of greenhouse emissions to the atmosphere has become mandatory and in the future will become more and more restrictive [1,2]. The combustion of fossil fuels for the transportation is a major contribution to the greenhouse gases and emissions of other pollutants and it is estimated that about 24% of the world-wide CO_2 emissions are caused by land, maritime and aeronautic transports [2,3]. A way to reduce these emissions is to drive this sector in the direction of "more electrified vehicles" (MEV) and currently the most promising technology to do so is with fuel-cells [4–6]. The implementation of a fuel-cell system on-board a vehicle, in particular as an auxiliary power unit (APU) on fossil fuels based vehicles, would increase energy efficiency and reduce of the fuel consumption.

A new fuel processing technology by partial dehydrogenation (PDh) of liquid hydrocarbons is gathering growing interest for hydrogen generation purposes. PDh leads to high purity, CO-free hydrogen, without denaturing the starting hydrocarbons which can be recycled to the fuel tanks. On-board hydrogen production via partial dehydrogenation of kerosene has emerged as an innovative way to produce hydrogen for aviation applications with an increasing number of publications on this subject. The most promising catalyst for this reaction uses Pt alloys supported on mesoporous materials. As first reported by Resini et al. [7], catalytic reaction of kerosene at 350 °C, 5 bar pressure over 5% wt. Pt-1% wt. Sn/γ-Al_2O_3 and 5% wt. Pt-1% wt. Sn-1% wt. Na/γ-Al_2O_3, obtained by impregnation of alumina pellets produces high purity H_2 (90–96% vol.), containing mainly impurities of CH_4 and light hydrocarbons. Better results in terms of purity and hydrogen productivity were subsequently reported by Lucarelli et al. [8,9] also using bimetallic Pt–Sn catalysts. In previous work we have described the possibility of further increasing the process performance either by enhancement of the Pt–Sn/γ-Al_2O_3 system by modification of the support [10] or by the modification of the active phase by addition of a third metal component [11], or by pretreatment of the kerosene feed [12].

Considering the encouraging results obtained in PDh of kerosene, we decided to carry out a feasibility study of the partial dehydrogenation of gasoline and diesel fuels. Since no previous example of partial dehydrogenation of gasoline and diesel were found in the literature we decided, in a first stage, to use fuel surrogates but without presence of sulfur components, in order to better understand the reactivity and explain the mechanisms of reaction and catalyst deactivation, while avoiding sulfur components well known to have a significant impact on catalyst deactivation. This

* Corresponding author. Fax: +33 0 467143304.
E-mail address: melanie.taillades-jacquin@univ-montp2.fr (M. Taillades-Jacquin).

http://dx.doi.org/10.1016/j.apcatb.2015.12.015
0926-3373/

Table 1
Fuel surrogate compositions.

Gasoline A	Gasoline B	Diesel A	Diesel B
N-heptane 13.5%	*N*-heptane 15%	*N*-hexadecane 23.5%	*N*-hexadecane 24%
Iso-octane 37.5%	*Iso*-octane 38%	Iso-octane 19%	*Iso*-octane 19%
Cyclohexane 9%	Cyclohexane 10%	Butyl-cyclohexane 27%	Butyl-cyclohexane 27%
Cyclohexene 6%	Cyclohexene 7%	Butyl-benzene 23%	Butyl-benzene 23%
Toluene 30.5%	Toluene 30%	1-Me-napthalene 7.5%	Tetralin 7%
Ethanol 3.5%			

experimental work has as objective the evaluation of the feasibility of the hydrogen production on-board vehicles that rely on gasoline and diesel for their propulsion.

2. Experimental

2.1. Catalyst preparation

The catalyst used for partial dehydrogenation reactions was prepared via incipient wetness impregnation, using the same procedure than in our previous work [10]. The alumina support was prepared via sol–gel method using $AlCl_3$ (Sigma–Aldrich) a sucrose non-surfactant template, NH_4OH for pH regulation and de-ionized water. The mole ratio used for the synthesis of the γ-Al_2O_3 support was 1:0.5:75 for Al:sucrose:H_2O. The resulting gel was heated at 60 °C until dry and calcined at 600 °C for 6 h. Aqueous solutions of $H_2PtCl_6{\cdot}6H_2O$ (*Alfa Aesar*) and $SnCl_2{\cdot}2H_2O$ (*Acros*), in a ratio 1% wt. Pt and 1% wt. Sn (mol. ratio Pt/Sn = 0.61) were used to co-impregnate the alumina support. The tin precursor was first dissolved in 1 M HCl and then mixed with the platinum salt solution upon which the solution turns red–brown due to the formation of a $[PtCl_2(SnCl_3)_2]^{2-}$ complex. It is reported that the procedure of Pt–Sn co-impregnation leads to a higher amount of PtSn alloy formation that favors catalyst stability [13,14]. After drying the impregnated catalyst overnight at 80 °C, it was thermally treated in air at 120 °C for 2 h and then at 560 °C for 2 h (ramp rate 2 °C min^{-1}).

2.2. Fuel surrogates

The composition of the four fuel surrogates used in this work is given in Table 1. The two gasoline surrogates A and B are based on the formulation proposed by Pera et al. [15] and comprises a five component mixture of *n*-heptane, *iso*-octane, cyclohexane, cyclohexene and toluene. The difference between gasoline A and B is that the former also contains ethanol. The two diesel surrogates are formulated on the basis of the studies carried out by Pitz et al. [16]. Both are a mixture of *n*-hexadecane, *iso*-octane, butyl-cyclohexane and butylbenzene but differ by the compound representative of the bi-cyclic hydrocarbons class: 1-methyl-naphthalene for diesel A and tetralin for diesel B.

2.3. Catalyst characterization

Adsorption–desorption of N_2 was carried out at −196 °C with an *ASAP2020* system from *Micromeritics*. Samples were out-gassed at 200 °C for 8 h under a vacuum of 66.7 Pa. Specific surface area was calculated using the BET (Brunauer, Emmett and Teller) method and pore size distribution using the BJH (Barrett, Joyner, Halenda) method using the *ASAP2020* implemented software; pore volume values are relative to the condensation point at $P/P^0 = 0.99$. The acidity of the materials was studied by NH_3 temperature programmed desorption (NH_3-TPD), using an *Autochem 2910* automatic system from *Micromeritics*. Samples were heated to 550 °C in a He flow of 30 ml min^{-1} (ramp rate 5 °C min^{-1}) then cooled to 100 °C. A flow of 20 ml min^{-1} NH_3 was passed over the samples for 1 h, then replaced with He at 100 °C for 1 h. NH_3 was thermally desorbed up to 600 °C with a heating ramp of 10 °C min^{-1} and the signal was recorded using a TC (thermal-conductivity) detector. The apparatus was calibrated using $Ni(NH_3)_6Cl_2$. H_2 temperature programmed reduction (H_2-TPR) war performed in an *Autochem 2910* apparatus. The samples were oxidized in synthetic air (30 ml min^{-1}; 500 °C, 5 °C min^{-1}). After cooling to 50 °C, a 30 ml min^{-1} flow of H_2 (5%)/N_2 mixture was passed over the sample, which was then heated at 10 °C min^{-1} up to 700 °C, recording the H_2 consumption with a TC detector. H_2 chemisorption was performed in an *Autochem 2910* apparatus. The samples were heated in air flow (30 ml min^{-1}; 500 °C, 5 °C min^{-1}) and then reduced with a H_2(5%)/N_2 mixture at 350 °C. Desorption of physisorbed hydrogen was carried out in N_2 flow at 380 °C for 1 h. Pure H_2 pulse adsorption was recorded at 40 °C. The stoichiometry assumed for the dispersion calculation was $Pt/H_2 = 2$ and for the particles size calculation the shape considered was a hemisphere. The amount of chemisorbed hydrogen is determined from the hydrogen pulse peaks. Thermogravimetric analyses of used catalysts were performed using a *Netzsch* STA409TP TG/DTA system, working in dynamic-air flux mode. Before the analysis, samples were out-gassed overnight to eliminate any residue of volatile products in the samples. The thermal program (1 h standby at 60 °C then heating up to 800 °C), was performed in a flow of synthetic air of 50 ml min^{-1}, with a ramp of 5 °C min^{-1}. CNHS elemental analysis on spent catalysts was performed with a *ThermoFinnigan Flash EA1112* automatic analyzer.

2.4. Catalytic tests

The PDh reactions on fuel surrogates were performed in a stainless steel fixed-bed tubular reactor. Before the reaction, the catalyst was oxidized in synthetic air flow (55 ml min^{-1}) at 500 °C and reduced in a H_2/Ar flow (55 ml min^{-1}–4:6 v/v) at 350 °C and atmospheric pressure for 2 h. In order to start the reaction the fuel was fed with a volumetric pump (*Shimatzu* LC20AD—0.53 ml min^{-1}) to the evaporator and then vaporized fuel, for the reactions carried out with recycle simulation, was mixed with a 7% vol. of H_2 before entering the reactor containing pelletized catalyst (d = 1–0.85 mm; $V_{cat.bed}$ = 1.8 cm^3; mass average ≈1 g). These flows were regulated in order to obtain a contact time τ = 2 s (calculated at standard temperature and pressure). A scheme of the reaction rig is shown in Fig. 1. After condensation of the partially dehydrogenated fuel, hydrogen production (NL h^{-1} kg_{cat}^{-1}) was calculated from measurement of the gas out-flow with a digital mass flow meter (*Brooks 5860S1 Smart II* mass flow meter), and the data processed with *LabView 8.2* instrumentation software. Hydrogen production was calculated following the Eq. (1):

$$H_2 \text{ production rate} = \frac{\text{Produced gas outflow (NL/h)} - \text{Hydrogen recycle (NL/h)}}{m_{cat}\,(\text{kg})} \quad (1)$$

Hydrogen purity was analyzed with an *Agilent 7890A* gas chromatograph equipped with a dual column system. A *HP-PLOT molesieve 5A column* connected to a Thermal Conductivity Detector (TCD) was used to analyze the composition of the gas produced by the reaction (hydrogen, methane, propane) and *a HP-PLOT/Q*

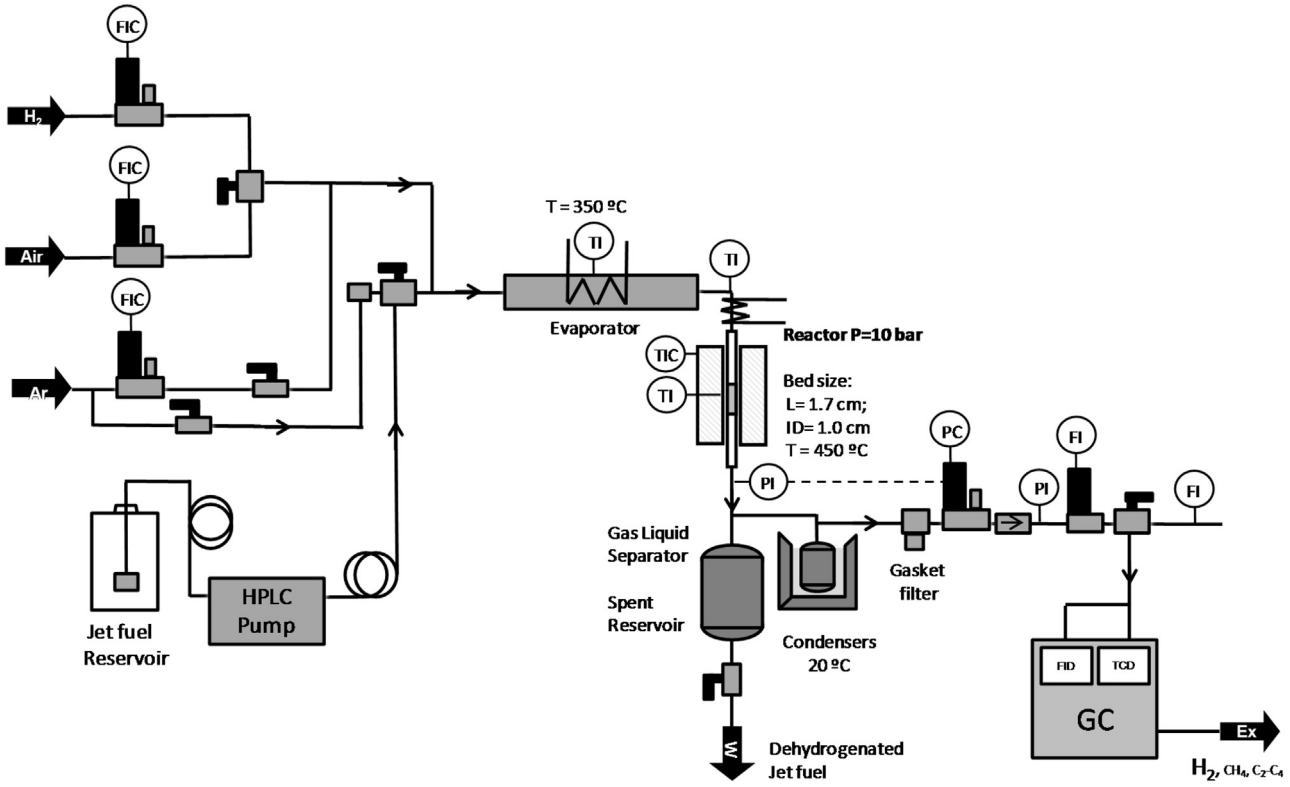

Fig. 1. Test rig schematics.

column with a Flame Ionization Detector (FID) to analyze the traces of light hydrocarbons (C4–C5) present in the gas stream. Hydrogen yield is calculated as ratio between hydrogen produced and total amount of hydrogen in the fuel used for the reaction (w/w). Catalyst lifetime is calculated only for the reaction of 6 h by linear extrapolation of the H_2 productivity curves between 180 and 360 min (at the steady-state) of TOS (time on stream). The lifetime is defined as the point in which hydrogen production reaches zero.

3. Results and discussion

3.1. Catalyst characterization

The catalyst characterization has already been discussed in our previous work [10], and Table 2 here, summarizes the main properties of the material. The surface area of the alumina support of 245 $m^2\ g^{-1}$ slightly decreases after the co-impregnation of Pt–Sn to a value of 226 $m^2\ g^{-1}$. This reduction of specific area is accompanied by a slight decrease in the pore volume, while the pore diameter distribution remains centered at 4.5 nm both for the support and the catalyst. The NH_3-TPD profiles reported in Fig. 2 indicate that the total acidity is reduced after the Pt and Sn co-impregnation, from 124 $\mu mol_{NH3}\ g^{-1}$ to 96 $\mu mol_{NH3}\ g^{-1}$. This effect, consistent with what is observed from the reduction profile of the catalyst, suggests the formation of Sn aluminate species on the acid sites of the alumina [17,18]. The ratio between strong and weak acid sites is not modified by the impregnation and for both samples, a prevalence of weak acid sites is observed. The reduction profile of the catalyst is reproduced in Fig. 3. The signal results in a main asymmetric peak of hydrogen uptake with a maximum at ≈250 °C. This main contribution is attributed to the reduction of Pt oxide and possibly to the reduction of Sn oxide. The reduction of Pt species in strong interaction with the alumina support is reported to occur at 200–300 °C [19,20] and the reduction of Sn(IV) to Sn(II) at 200–300 °C in the presence of Pt catalyzing the reduction, leading to the formation of Pt_xSn [21–24]. The hydrogen uptake observed above 350 °C, causing the asymmetry observed in the hydrogen uptake peak, is attributed to the reduction of Sn oxides, possibly Sn aluminates species [23,24], in strong interaction with the support. The values of metal dispersion and average metal particle size, reported in Table 2, are calculated from the H_2 chemisorption analysis. The 88% obtained is a metal dispersion, in line with similar analysis carried out on Pt/Al_2O_3 and $Pt–Sn/Al_2O_3$ catalysts [25,26]. It has to be considered though, that the main factor responsible for hydrogen adsorption at room temperature in chemisorption measurements is the fraction of unalloyed Pt, rather than the Pt in alloy with Sn. As consequence, when calculating the average particle size from the H_2-chemisorption data, the result cannot be directly related to the real size of metal clusters (composed by multiple metal species that can or cannot adsorb H_2), but is a index of the accessibility of Pt atoms [20].

3.2. Catalytic partial dehydrogenation of gasoline surrogates

Fuels like gasoline and diesel are complex mixtures of hydrocarbons containing more than 200 different compounds (depending

Table 2
Summary of catalyst properties.

	Surface Area (m^2/g)	Pore volume(cm3/g)	Pore diameter (nm)	Acidity ($\mu molNH_3$/g)	Metallic Dispersion (%)	Particle size (nm)
γ-Al_2O_3	245	1.6	4.5	125	/	/
Pt–Sn/γ-Al_2O_3	226	1.3	4.5	96	88	1,28

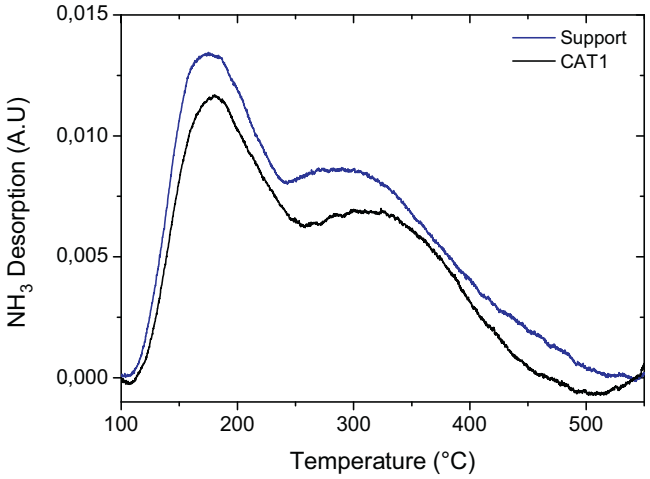

Fig. 2. NH3-TPD profiles for the support and Pt–Sn/γ-Al_2O_3 catalyst.

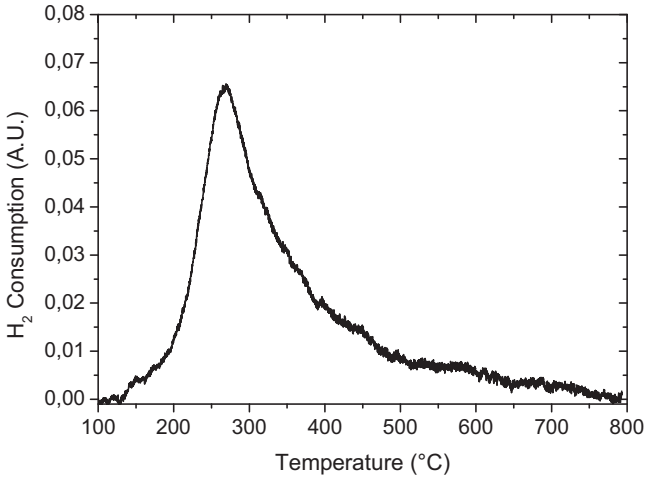

Fig. 3. H2-TPR profile for Pt–Sn/γ-Al_2O_3 catalyst.

on the origin of the native oil and the fraction considered). This would make very complicated the separation and identification of all the components. As consequence this study has been carried out using surrogate fuels in order to facilitate the understanding of the reaction mechanisms and the calculation of yield, conversion and selectivity for the different compounds. The fuel surrogates have been formulated to be the most representative as possible of the actual fuels, in terms of chemical composition and thermodynamics properties [15,16] but without sulfur components. Fig. 4 shows the comparison between the hydrogen productivity obtained with the two different gasoline surrogates at 350 °C, 0.1 MPa, $\tau = 2$ s without hydrogen recycle. The surrogate A contains ethanol and has been used in order to investigate the possibility of producing hydrogen from new generation ethanol-containing bio-gasoline by the PDh reaction.

The average hydrogen productivity for the gasoline surrogate B is around 1600 NL h^{-1} kg_{cat}^{-1}, while for the surrogate A, containing ethanol, the average productivity is considerably lower with 900 NL h^{-1} kg_{cat}^{-1}. The presence of ethanol seems to be detrimental for the catalyst activity at these reaction conditions.

The degree of conversion of the two surrogates after reaction, shown in Fig. 5, gives another indication of the effect of the ethanol on the reactivity. For the surrogate B it is observed the almost complete conversion of cyclic hydrocarbons (cyclohexane and cyclohexene) is observed with high selectivity to the

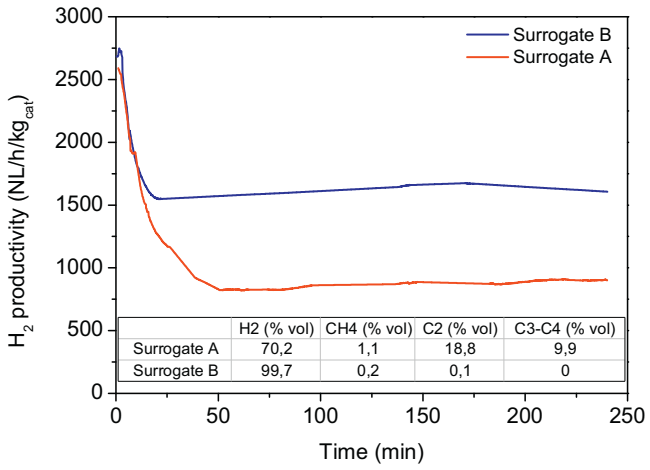

	H2 (% vol)	CH4 (% vol)	C2 (% vol)	C3-C4 (% vol)
Surrogate A	70,2	1,1	18,8	9,9
Surrogate B	99,7	0,2	0,1	0

Fig. 4. H_2 productivity and purity obtained using gasoline surrogates feeds at 350 °C, 0.1 MPa and $\tau = 2$ s.

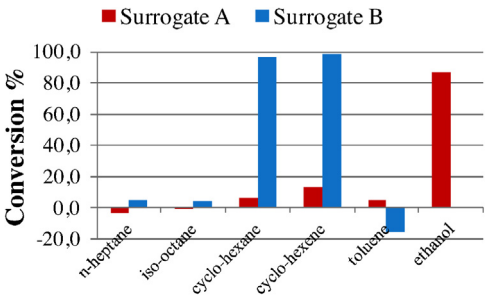

Fig. 5. Conversion of components of gasoline surrogates at 350 °C, 0.1 MPa and $\tau = 2$ s.

corresponding aromatic compound (benzene). The paraffins (*n*-heptane and *iso*-octane) show a low reactivity and they are converted to toluene via dehydrocyclization (see below) while the aromatic component (toluene) is unreactive. This behavior is consistent with the results in the literature for the partial dehydrogenation of kerosene with high reactivity of the cyclic hydrocarbons (which produce the majority of the hydrogen) and low conversion for paraffins and aromatics [8,9,27].

When ethanol is present (gasoline surrogate A), a considerable difference in the reactivity is observed: with the exception of the ethanol that has a conversion of more than 80%, the conversion of the other compounds drops below 10% even for the cyclic hydrocarbons which should be the most reactive.

In terms of hydrogen purity (Fig. 4) a considerable difference is noted between gasoline A (with ethanol) and gasoline B, with values of 70.2% vol. and 99.7% vol. respectively. In the case of gasoline B the main impurity is methane (0.2% vol.), while for the surrogate A the impurities are C_2 light hydrocarbons (18.8% vol.), C_3–C_5 (9.9% vol.) and methane (1.1% vol.). The high amount of the C_2 impurities observed for the reaction with gasoline A could be due to the dehydration of ethanol to ethene and water catalyzed by the acid sites of the alumina [28,29]. The ethene formed can subsequently polymerize and form a carbon coke that covers the active phase, causing the rapid deactivation and low conversion measured for the reaction. This hypothesis, that would explain the differences observed between the reactivity of the two gasoline surrogates, is also corroborated by TGA/DTA analyses performed on the spent catalysts.

The DTA profiles of spent catalysts after reaction with the two gasoline surrogates are shown in Fig. 6. The curves represent the combustion of the carbon coke deposited on the catalyst during the

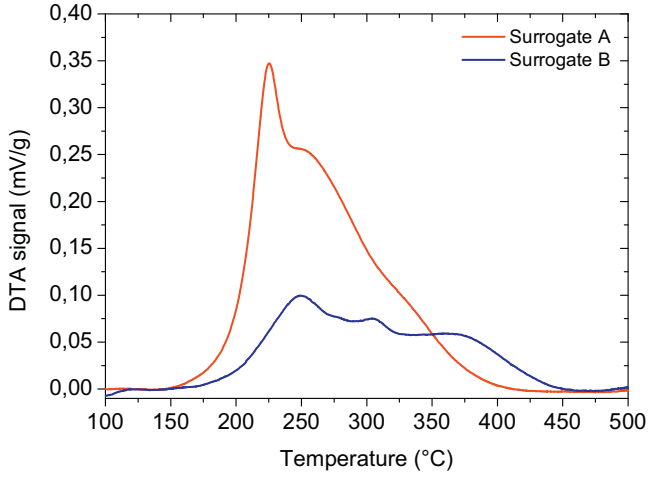

Fig. 6. DTA signal given by the spent Pt–Sn/γ-Al_2O_3 catalyst after reaction with gasoline surrogates.

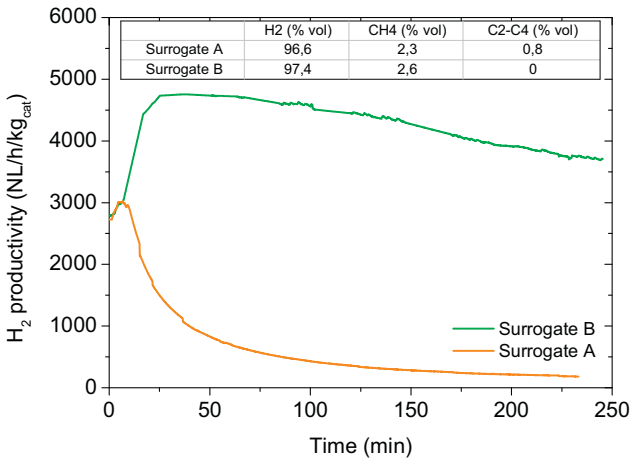

Fig. 7. H_2 productivity and purity obtained using diesel surrogates feeds at 450 °C, 0.1 MPa and τ = 2 s.

partial dehydrogenation reaction. For the gasoline A, a significantly higher amount of coke is measured and the most important difference between the DTA signals is in the contribution observed at low temperature (200–250 °C). This contribution, that is predominant for the gasoline A, can be attributed to the carbon coke deposited on the metal particles via polymerization of the ethene formed via ethanol dehydration.

3.3. Catalytic partial dehydrogenation of diesel surrogates

The two different diesel surrogates differ by the component representative of the bicyclic hydrocarbons class. This choice has been made in order to study of the effect of free radicals formation in the reaction environment during the PDh reaction. Fig. 7 shows the hydrogen productivity for diesel A and B at 450 °C, 0.1 MPa, τ = 2s without hydrogen recycle.

The PDh of diesel surrogate B leads to a high average hydrogen productivity of 4500 NL h^{-1} kg_{cat}^{-1} with a purity of 97.4% vol., while for the diesel A the average is below 500 NL h^{-1} kg_{cat}^{-1} with a purity of 95.8% vol. It is also observed that for the diesel A, the deactivation of the catalyst is extremely rapid with almost complete deactivation already at 4 h TOS.

The conversions calculated for the reaction with the two fuels, shown in Fig. 8, are consistent with the amount of hydrogen generated. For diesel A, the conversion is low for all the compounds with values around 10%, while for diesel B the reactivity is similar to what observed for the PDh of kerosene and gasoline B, with high conversion of cyclic hydrocarbons (butylcyclohexane 80%, tetralin 100%) and almost no conversion of paraffins and aromatics.

The considerable gap in productivity and conversions between the two diesel surrogates is due to the presence of a different compound representing the bicyclic hydrocarbons: 1-methylnaphtalene in diesel A and tetralin in diesel B. It is known that 1-methyl-naphthalene can easily form dibenzyl radicals at the operating conditions of the partial dehydrogenation, which can subsequently undergoes polycondensation leading to the formation of coke [30,31]. This hypothesis is consistent with the results obtained analyzing the spent catalysts via TGA/DTA.

The DTA curves for the spent catalysts after reaction with the diesel surrogate A and B are shown in Fig. 9. The amount of coke formed with surrogate A is more than threefold that of surrogate B, with a 13 wt%. This difference seems to be mainly related to the contribution observed at 400–500 °C in the DTA curve of the spent catalyst from surrogate A, and this peak can be therefore be attributed to the carbon coke formed via radical reactions from the 1-methylnaphtalene.

In conclusion from this section, the results obtained suggest that, the catalyst Pt/Sn-Al_2O_3 is not appropriate for the partial dehydrogenation of gasoline that contains ethanol. For diesel, the reaction efficiency depends on the presence of specific bi-cyclic hydrocarbons, which can lead to the formation of free radicals that are detrimental to the catalyst since at the origin of polymerization reactions leading to coke formation. As consequence it was decided to pursue the preliminary studies with gasoline B and diesel B.

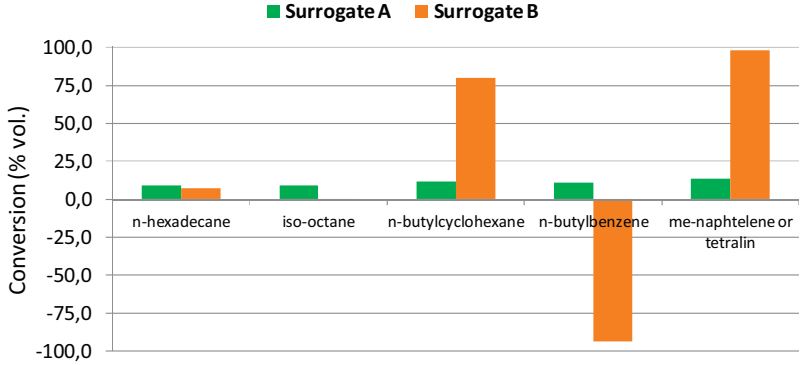

Fig. 8. Conversion of diesel surrogate components at 450 °C, 0.1 MPa and τ = 2 s.

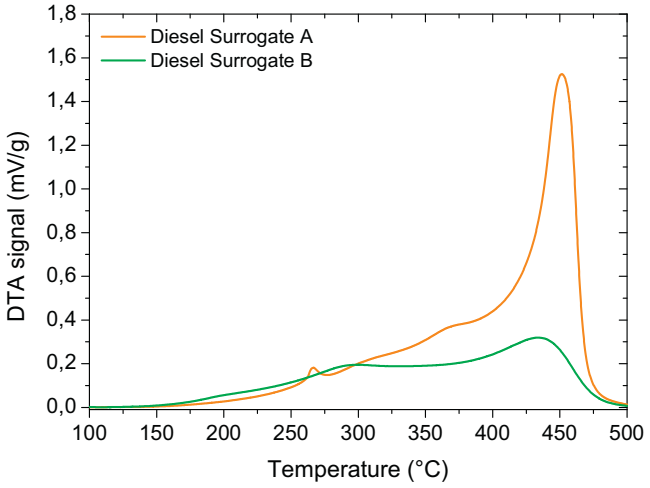

Fig. 9. DTA signal of the spent Pt–Sn/γ-Al_2O_3 catalyst after reaction with diesel surrogates.

3.4. Effect of the temperature reaction and of the hydrogen recycling on the hydrogen productivity

Experiments performed at different temperatures and $P = 0.1$ MPa, $\tau = 2$ s with gasoline B and diesel B are shown in Fig. 10. For both gasoline B and diesel B, a considerable increase in productivity is observed on increasing the temperature from 350 °C to 400 °C. A further increase in productivity is achieved for diesel B at 450 °C, while for the gasoline B this effect is not observed. In terms of hydrogen purity (Fig. 11), the gasoline and diesel surrogates display similar dependence temperature, with values above 99% vol. at 350 °C and 400 °C and a decrease of purity at 450 °C with values of 97.5% vol. and 97.4% vol. The main impurities are CH_4 and traces of light hydrocarbons (C_2–C_4).

The conversions and selectivity as a function of the reaction temperature with gasoline B and diesel B feeds are reported in Figs. 12 and 13 respectively. The behavior observed is similar for both fuels displaying high conversion for the more reactive cyclic or bi-cyclic hydrocarbons and low conversion for the others hydrocarbons.

With the gasoline surrogate B, cyclohexane and cyclohexene are converted with 100% selectivity to benzene at all temperatures. Cyclohexene shows complete conversion at the three temperatures examined, while cyclohexane requires a temperature of 400 °C in order to reach 100% conversion. Toluene is not reactive and further more displays a negative conversion as it is produced via dehydrocyclization of *n*-heptane and *iso*-octane. The last two compounds have low conversion at 350 °C (1.5% and 2.9% respectively) which increases with the temperature. The selectivity to toluene though is lowered with increasing temperature, in particular at 450 °C highlighting that cracking reactions became more favored with respect to the dehydrocyclization pathway. In diesel surrogate B, the cyclic hydrocarbons butylcyclohexane and tetralin are converted with 100% selectivity, at all temperatures, to butylbenzene and naphthalene respectively. The reactivity of butylcyclohexane is more dependent on temperature if compared to what is observed for cyclohexane in gasoline B. The conversion of butylcyclohexane, that is only 25.3% at 350 °C, is considerably increased at 400 °C and 450 °C with values of 74.1% and 79.8% respectively. Tetralin is the compound that is more easily dehydrogenated, with a conversion that is close to 100% already at the lowest temperature employed (350 °C).

The optimal temperature for the PDh of both gasoline and diesel seems to be 400 °C. At this temperature the best compromise between the feed conversion and selectivity towards the dehydrogenation reaction is observed, while secondary reactions like cracking are limited, allowing the production of hydrogen with a purity of over 99% vol.

The effect of the introduction of hydrogen recycling has been investigated for gasoline B and diesel B carrying out catalytic reactions at 400 °C, 0.1 MPa, $\tau = 2$ s and 7% vol. of hydrogen in the feed together with the fuel vapor. In Fig. 14 are reported the hydrogen productivity curves for gasoline B and diesel B.

The introduction of the hydrogen recycle has a similar effect for both fuel surrogates with a slight reduction of the hydrogen productivity, accompanied by an increase of the extrapolated lifetime of the catalyst. The lifetime is defined as the point in which hydrogen production reaches zero. The increase in the lifetime observed for gasoline B though is significantly more remarkable than for diesel B, with an increase of the lifetime of more than threefold from 118 h without H_2 recycle to 376 h with the recycle. The increase in lifetime for diesel B on the other hand is only of few hours. For both the fuel surrogates there is less carbon coke deposited in the course of the reaction when the recycle is introduced.

In terms of the hydrogen purity (Fig. 15) the recycling does not affect considerably the distribution of the products. For the gasoline and diesel surrogates, a slight drop of the purity of 0.4% vol. and 0.1% vol. are observed respectively with a corresponding increase in the concentration of methane and light hydrocarbons (C_1–C_4). The introduction of the hydrogen recycle slightly increases the hydrogen partial pressure leading to an increase of hydrogenolysis reactions, which can explain the change in the purity of the hydrogen produced. The conversion and selectivity (Figs. 16 and 17) do not display significant changes with the introduction of the recycle.

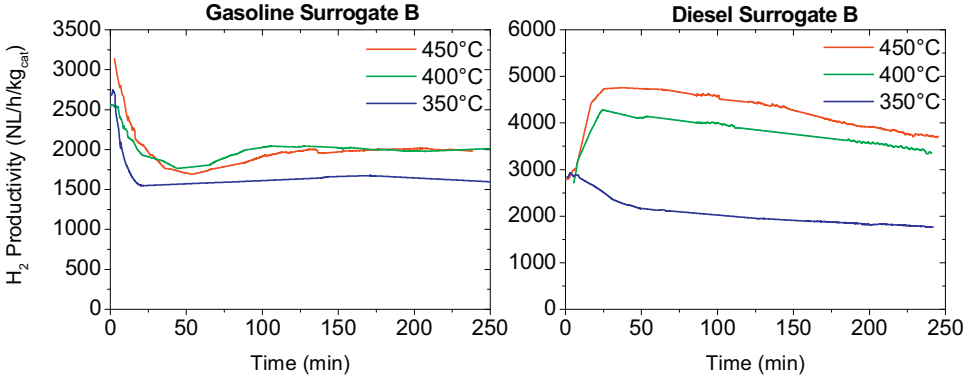

Fig. 10. Dependence of H2 productivity on reaction temperature using gasoline B and diesel B.

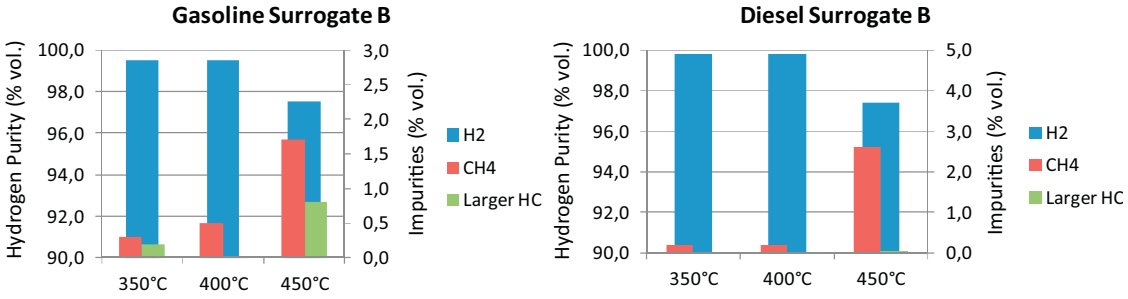

Fig. 11. Dependence of H_2 purity on reaction temperature using gasoline B and diesel B.

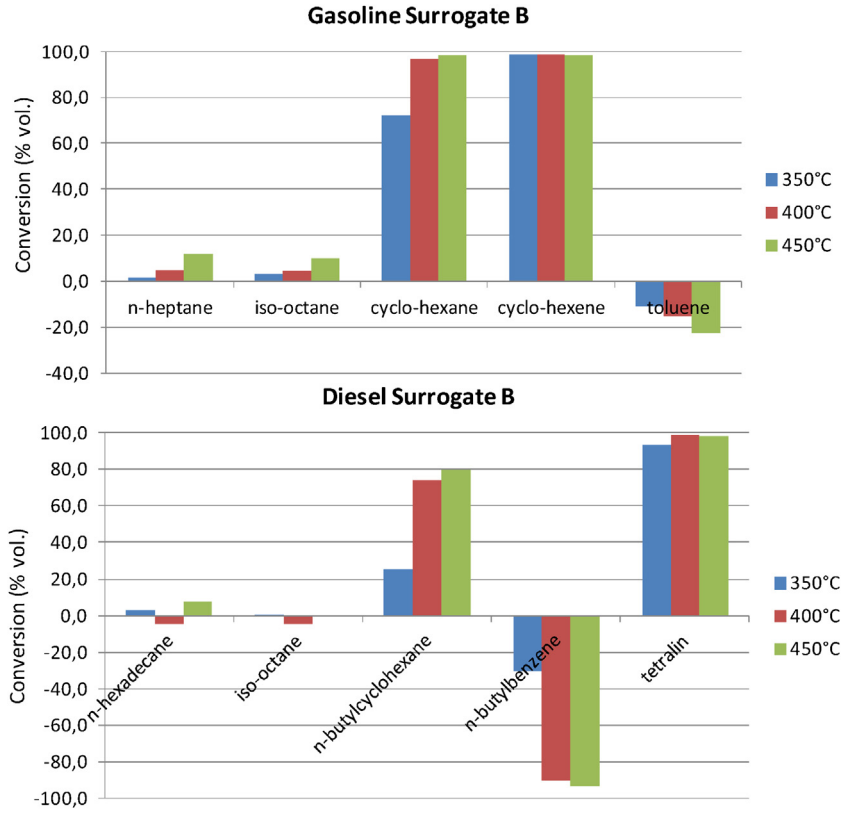

Fig. 12. Dependence of conversion of gasoline B and diesel B components on reaction temperature.

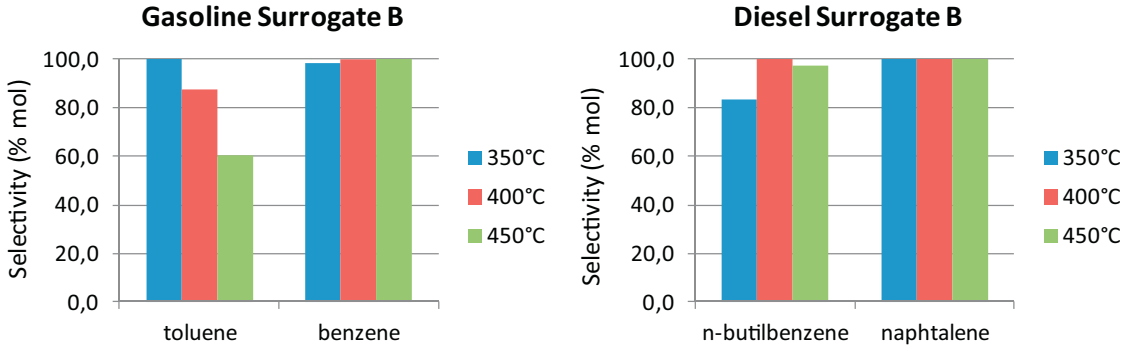

Fig. 13. Dependence of selectivity on reaction temperature for gasoline B and diesel B surrogates.

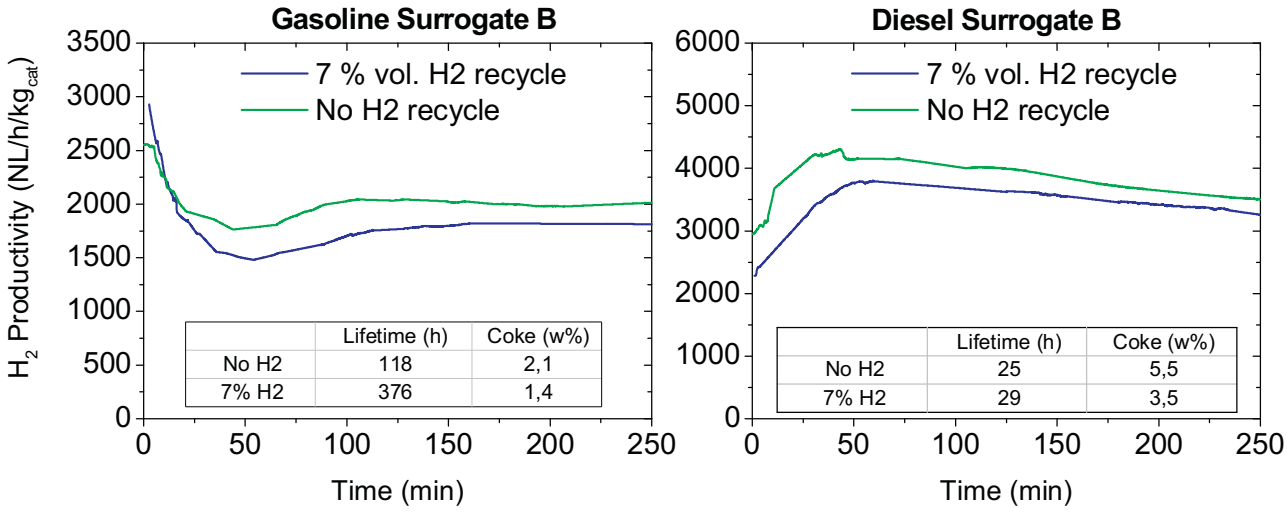

Fig. 14. Effect of recycle on H_2 productivity and catalyst lifetime using gasoline B and diesel B surrogate feeds.

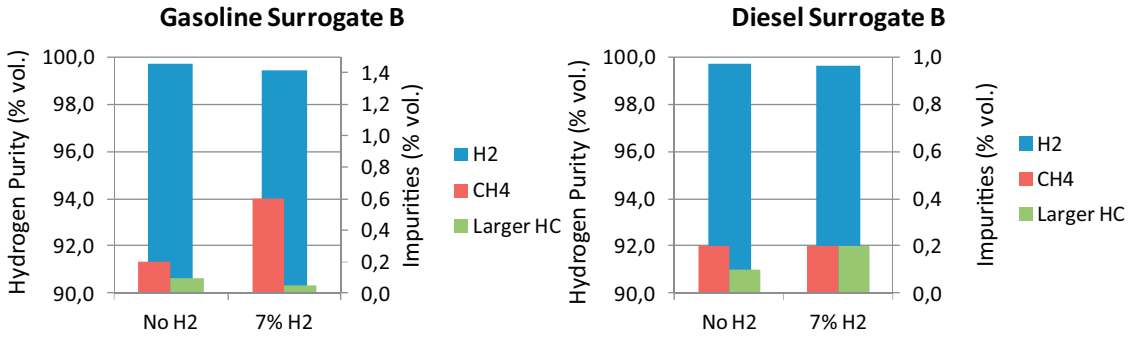

Fig. 15. Effect of recycle on H_2 purity for gasoline B and diesel B.

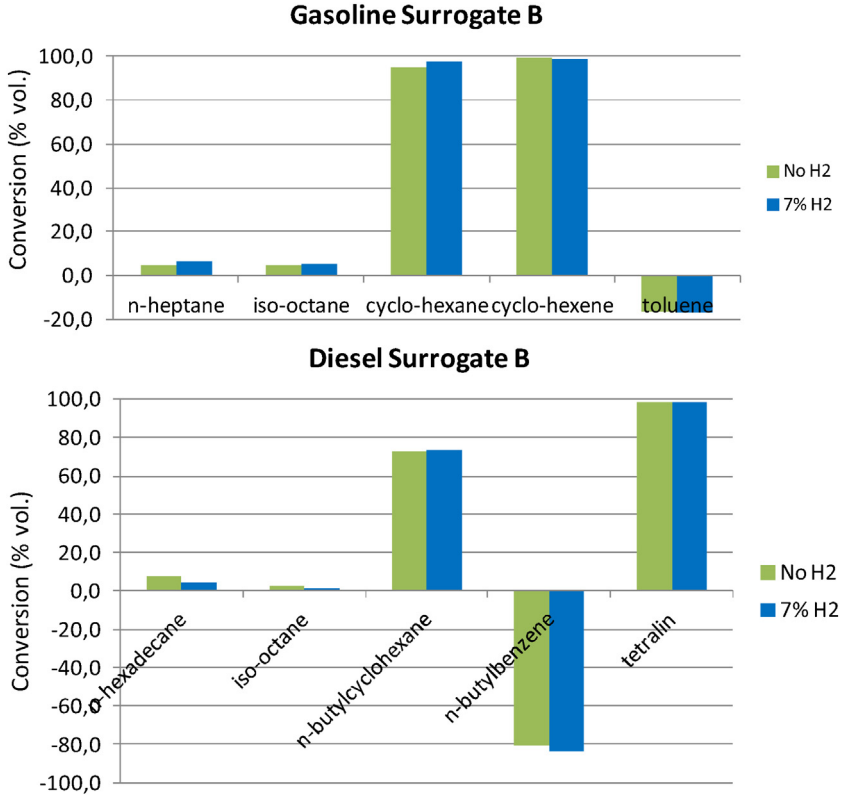

Fig. 16. Effect of recycle on conversion of gasoline B and diesel B.

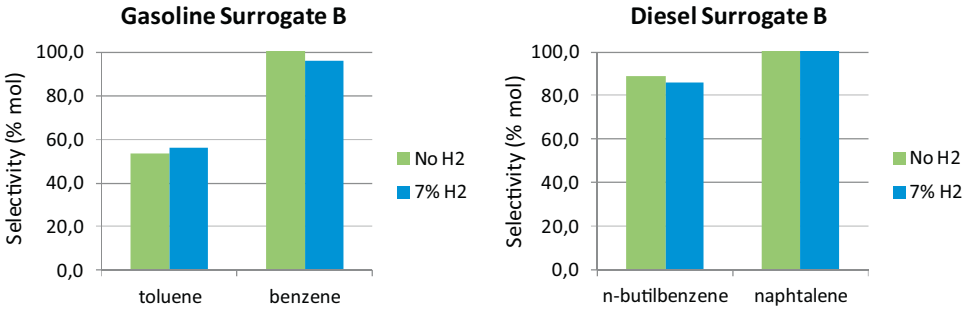

Fig. 17. Effect of recycle on selectivity for gasoline B and diesel B.

4. Conclusion

The catalytic partial dehydrogenation of fuels for high purity hydrogen generation is a promising technology for feeding fuel-cells systems on-board vehicles. The optimal reaction conditions indentified for the gasoline and diesel surrogates are 400 °C, 0.1 MPa, $\tau = 2$ s and 7% vol. of hydrogen recycle. The PDh of gasoline allowed an average hydrogen production of 1800 NL h^{-1} kg_{cat}^{-1} with a purity of over 99% vol. and projected lifetime of 376 h. The study highlighted that the catalyst used is very sensitive to the presence of ethanol in the feedstock, so the application of this process to new generation bio-gasoline (containing a high amount of bio-ethanol) it would not be possible using this catalyst. The PDh of diesel provided an average hydrogen production of 3500 NL h^{-1} kg_{cat}^{-1}, of purity over 99% vol. and a lifetime of 29 h. The study highlighted that the catalyst is strongly affected by the presence of a specific type of bicyclic hydrocarbon in the surrogate (1-methylnaphthalene) that cause the formation of free radicals and polymerization reactions in the reaction environment that obstruct access to catalyst sites. The application of the PDh to a diesel vehicle is consequently limited by the fuel composition and catalyst lifetime. The amount of hydrogen produced is encouraging, but a further improvement of the catalyst is required in order to obtain satisfying results in terms of the catalyst durability.

References

[1] IEA, Key World Energy Stat, I. E. A., 2012.
[2] L. Bernstein, P. Bosch, O. Canziani, et al., Climate Change 2007: Summary for Policymakers (2007).
[3] ITF, I. T. F, Reducing transport ghg emissions: opportunities and costs (2009).
[4] D. Carter, J. Wing, Fuel Cell Ind. Rev. (2013).
[5] U.S.DOE, Hydrogen production and delivery: summary of annual merit review of the hydrogen production and delivery program (2013).
[6] U.S.DOE, Hydrogen, Fuel Cells & Infrastructure Technologies Program—multiyear research, development and demonstration plan (2010).
[7] C. Resini, C. Lucarelli, M. Taillades-Jacquin, K.-E. Liew, I. Gabellini, S. Albonetti, D. Wails, J. Roziere, A. Vaccari, D. Jones, Int. J. Hydrog. Energy 36 (2011) 5972–5982.
[8] C. Lucarelli, S. Albonetti, A. Vaccari, C. Resini, G. Taillades, J. Roziere, K.-E. Liew, A. Ohnesorge, C. Wolff, I. Gabellini, D. Wails, Catal. Today 175 (1) (2011) 504–508.
[9] C. Lucarelli, G. Pavarelli, C. Molinari, S. Albonetti, W. Mista, D. Di Domenico, A. Vaccari, Int. J. Hydrog. Energy 39 (3) (2014) 1336–1349.
[10] Á. Reyes-Carmona, E. Gianotti, M. Taillades-Jacquin, G. Taillades, J. Rozière, E. Rodríguez-Castellón, D. Jones, J. Catal. Today 210 (2013) 26–32.
[11] E. Gianotti, Reyes-Carmona Á, M. Taillades-Jacquin, G. Taillades, J. Rozière, D. Jones, J. Appl. Catal. B Environ. 160–161 (2014) 574–581.
[12] E. Gianotti, Reyes-Carmona Á, K. Pearson, M. Taillades-Jacquin, G. Kraaij, A. Wörner, J. Rozière, D. Jones, J. Appl. Catal. B Environ. 176–177 (2015) 480–485.
[13] Zangeneh, S. Farnaz Tahriri Mehrazma, S. Sahebdelfar, Fuel Process. Technol. (2012).
[14] B.K. Vu, M.B. Song, I.Y. Ahn, Y.-W. Suh, D.J. Suh, W.-I. Kim, H.-L. Koh, Y.G. Choi, E.W. Shin, Appl. Catal. A Gen. 400 (1–2) (2011) 25–33.
[15] C. Pera, V. Knop, Fuel 96 (2012) 59–69.
[16] W.J. Pitz, C. Mueller, J. Prog. Energy Combust. Sci. 37 (3) (2011) 330–350.
[17] J.L. Ayastuy, M.P. González-Marcos, M.A. Gutiérrez-Ortiz, Catal. Commun. 12 (10) (2011) 895–900.
[18] V.A. Mazzieri, J.M. Grau, J.C. Yori, C.R. Vera, C.L. Pieck, Appl. Catal. A Gen. 354 (1–2) (2009) 161–168.
[19] A. Jahel, P. Avenier, S. Lacombe, J. Olivier-Fourcade, J.-C. Jumas, J. Catal. 272 (2) (2010) 275–286.
[20] S.M. Stagg, C.A. Querini, W.E. Alvarez, D.E. Resasco, J. Catal. 94 (1997) 75–94.
[21] B.K. Vu, M.B. Song, I.Y. Ahn, Y.-W. Suh, D.J. Suh, W.-I. Kim, H.-L. Koh, Y.G. Choi, E.W. Shin, Appl. Catal. A Gen. 400 (1–2) (2011) 25–33.
[22] S. He, C. Sun, Z. Bai, X. Dai, B. Wang, Appl. Catal. A Gen 356 (1) (2009) 88–98.
[23] D.L. Hoang, S.A.-F. Farrage, J. Radnik, M.-M. Pohl, M. Schneider, H. Lieske, A. Martin, Appl. Catal. A Gen. 333 (1) (2007) 67–77.
[24] S. Luo, N. Wu, B. Zhou, S. He, J. Qiu, C. Sun, J. Fuel Chem. Technol. 41 (12) (2013) 1481–1487.
[25] L.D. Sharma, M. Kumar, A.K. Saxena, M. Chand, J.K. Gupta, J. Mol. Catal. A 185 (2002) 135–141.
[26] M. Haneda, T. Watanabe, N. Kamiuchi, M. Ozawa, Appl. Catal. B Environ. 142–143 (2013) 8–14.
[27] K. Pearson, T. Käfer, G. Kraaij, A. Wörner, Int. J. Hydrog. Energy (2014) 1–12.
[28] R.A. Zotov, V.V. Molchanov, A.M. Volodin, A.F. Bedilo, J. Catal. 278 (1) (2011) 71–77.
[29] T. Zaki, J. Colloid Interface Sci. 284 (2005) 606–613.
[30] T. Kabe, A. Ishiara, E.W. Qian, I.P. Sutrisna, Y. Kabe, Coal and coal-related compounds—structures, reactivity and catalytic reactions Studies in Surface Science and Catalysis, vol. 150, Elsevier, 2004.
[31] C.M. Blanchard, M.R. Gray, ACS—Div. Fuel Chem. 42 (1997) 137–141.